PAPER *Special Section on Radio Access Techniques for 3G Evolution*

Joint Frequency-Domain Equalization and Despreading for Multi-Code DS-CDMA Using Cyclic Delay Transmit Diversity

Tetsuya YAMAMOTO[†a)], **Kazuki TAKEDA**[†], *Student Members*, *and* **Fumiyuki ADACHI**[†], *Fellow*

SUMMARY Frequency-domain equalization (FDE) based on the minimum mean square error (MMSE) criterion can provide a better bit error rate (BER) performance than rake combining. To further improve the BER performance, cyclic delay transmit diversity (CDTD) can be used. CDTD simultaneously transmits the same signal from different antennas after adding different cyclic delays to increase the number of equivalent propagation paths. Although a joint use of CDTD and MMSE-FDE for direct sequence code division multiple access (DS-CDMA) achieves larger frequency diversity gain, the BER performance improvement is limited by the residual inter-chip interference (ICI) after FDE. In this paper, we propose joint FDE and despreading for DS-CDMA using CDTD. Equalization and despreading are simultaneously performed in the frequency-domain to suppress the residual ICI after FDE. A theoretical conditional BER analysis is presented for the given channel condition. The BER analysis is confirmed by computer simulation.

key words: *DS-CDMA, frequency-domain equalization, cyclic delay transmit diversity*

1. Introduction

In next generation mobile communication systems, broadband data services are demanded. Since the mobile wireless channel is composed of many propagation paths with different time delays, the channel becomes severely frequency-selective. In a severe frequency-selective fading channel, the bit error rate (BER) performance significantly degrades due to inter-symbol interference (ISI) when single carrier (SC) transmission without equalization technique is used [1]. Direct sequence code division multiple access (DS-CDMA) using coherent rake combining is adopted to obtain the path-diversity gain in the third generation mobile communication systems for data transmissions of up to a few Mbps [2]. However, for data transmissions of higher than a few 100 Mbps, the BER performance of DS-CDMA with rake combining degrades severely [3]. Recently, it was shown that frequency-domain equalization (FDE) based on the minimum mean square error criterion (MMSE) can replace rake combining to significantly improve the BER performance of DS-CDMA [3]–[7].

To further improve the BER performance, the use of transmit diversity technique is effective. Recently, cyclic delay transmit diversity (CDTD) was proposed for multi-carrier transmissions [8], [9]. CDTD increases the number of equivalent propagation paths by transmitting the same data from different antennas after adding different cyclic delays, and hence can achieve large frequency diversity gain. CDTD can also be applied to DS-CDMA using MMSE-FDE and improve the BER performance in a weak frequency-selective fading channel [10]–[12]. In [10]–[12], after MMSE-FDE, the time-domain despreading is performed. However, the residual inter-chip interference (ICI) is present after MMSE-FDE and this limits the BER performance improvement of DS-CDMA using CDTD [13].

In this paper, we propose a joint use of FDE and despreading for single- and multi-code DS-CDMA using CDTD in the frequency-domain. For the case of single-code transmission, the maximal ratio combining (MRC) weight is derived. Joint FDE and despreading using the MRC weight does not produce the residual ICI at all and hence, provide better BER performance than the conventional MMSE-FDE. For the case of orthogonal multi-code transmissions, two types of MMSE weight are derived. The first MMSE weight (called the MMSE weight type 1 in this paper) minimizes the mean square equalization error at each frequency individually. The second MMSE weight (called the MMSE weight type 2 in this paper) minimizes the totality of mean square equalization errors at all frequencies for all multi-code streams.

The remainder of this paper is organized as follows. Section 2 introduces CDTD. In Sect. 3, the joint FDE and despreading is proposed and a theoretical conditional BER analysis is presented for the given channel condition. In Sect. 4, the achievable average BER performance in a frequency-selective fading channel is evaluated by Monte-Carlo numerical computation method using the derived conditional BER. The BER analysis is confirmed by computer simulation of the signal transmission. Section 5 offers the conclusion.

2. Cyclic Delay Transmit Diversity

2.1 Transmit Signal

The transmitter structure of multi-code DS-CDMA using CDTD is illustrated in Fig. 1. Throughout the paper, the chip-spaced discrete time representation is used. At the transmitter, a binary information sequence is data-modulated and then, serial/parallel (S/P)-converted to U parallel streams. The data symbol $\{d_u; u = 0 \sim U-1\}$ in the uth stream is spread by an orthogonal spreading code

Manuscript received August 25, 2008.
Manuscript revised December 25, 2008.

[†]The authors are with the Department of Electrical and Communication Engineering, Graduate School of Engineering, Tohoku University, Sendai-shi, 980-8579 Japan.
a) E-mail: yamamoto@mobile.ecei.tohoku.ac.jp

DOI: 10.1587/transcom.E92.B.1563

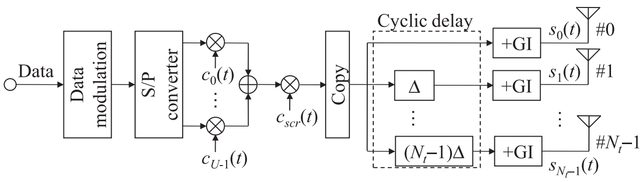

Fig. 1 Transmitter structure of multi-code DS-CDMA using CDTD.

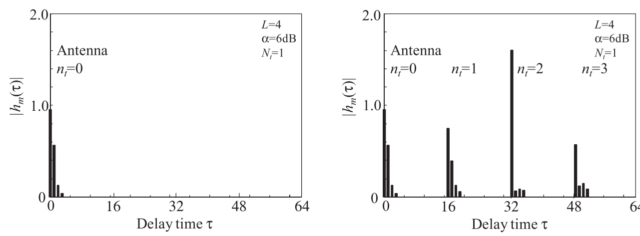

(a) N_t=1 (b) N_t=4

Fig. 2 Impulse response of the composite channel $h_m(\tau)$ when $\Delta = 16$.

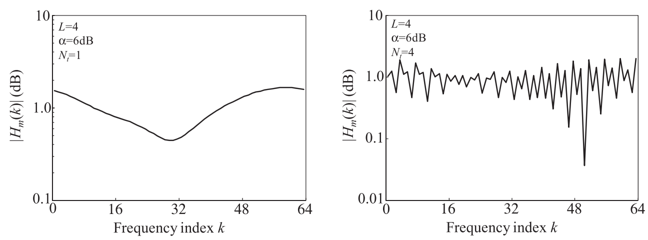

(a) N_t=1 (b) N_t=4

Fig. 3 Composite channel gain $H_m(k)$ when $\Delta = 16$.

$\{c_u(t); t = 0 \sim SF-1\}$ with the spreading factor SF. The resultant U chip streams are added and multiplied by a common scramble sequence $\{c_{scr}(t); t = \cdots, -1, 0, 1, \cdots\}$ to make the resultant multi-code DS-CDMA signal like white-noise. Considering the time interval of $t = 0 \sim SF-1$. The SF-chip block $\{s(t)\}$ is expressed using the lowpass equivalent representation as

$$s(t) = \sum_{u=0}^{U-1} d_u \cdot c_u(t) c_{scr}(t). \tag{1}$$

In CDTD, the same multi-code DS-CDMA signal is simultaneously transmitted from different antennas after adding different cyclic delays. N_t copies of $s(t)$ are generated and then, cyclic time delay $n\Delta$ is added before the transmission from the nth antenna ($n = 0 \sim N_t-1$). The transmitted chip sequence from the nth antenna, $\{s_n(t); t = 0 \sim SF-1\}$, can be expressed as

$$\begin{aligned} s_n(t) &= \sqrt{\frac{2E_c}{N_t T_c}} s((t-n\Delta) \mathrm{mod} SF) \\ &= \sqrt{\frac{2E_c}{N_t T_c}} \sum_{u=0}^{U-1} d_u \cdot \tilde{c}_u((t-n\Delta)\mathrm{mod} SF). \end{aligned} \tag{2}$$

where E_c and T_c denote the chip energy and the chip duration, respectively, and $\tilde{c}_u(t) = c_u(t)c_{scr}(t)$. The transmit signal power is reduced by a factor of N_t to keep the total transmit signal power intact. Finally, the last N_g chips of each block are copied as a cyclic prefix and inserted into the guard interval (GI) placed at the beginning of each block and the signals are transmitted.

2.2 Received Signal

In this paper, we consider N_r-antenna diversity reception. The signal transmitted from N_t antennas goes through different frequency-selective fading channels, each composed of L distinct paths. The received signal at the mth received antenna is a superposition of N_t transmitted signal and can be expressed as

$$\begin{aligned} r_m(t) &= \sum_{n=0}^{N_t-1}\sum_{l=0}^{L-1} h_l^{n\to m} s_n(t-\tau_l^{n\to m}) + \eta_m(t) \\ &= \sqrt{\frac{2E_c}{N_t T_c}} \sum_{n=0}^{N_t-1}\sum_{u=0}^{U-1} d_u \sum_{l=0}^{L-1} h_l^{n\to m} \tilde{c}_u((t-n\Delta-\tau_l^{n\to m})\mathrm{mod} SF) \\ &\quad + \eta_m(t), \end{aligned} \tag{3}$$

where $h_l^{n\to m}$ and $\tau_l^{n\to m}$ are respectively the complex-valued path gain and the time delay of the lth path between the nth transmit antenna and the mth receive antenna, and $\eta_m(t)$ is the zero-mean additive white Gaussian noise (AWGN) having the variance $2N_0/T_c$ with N_0 being the one-sided noise power spectrum density.

At the receiver, after the GI removal, SF-point fast Fourier transform (FFT) is applied to transform the received signal $\{r_m(t); t = 0 \sim SF-1\}$ into the frequency-domain signal $\{R_m(t); k = 0 \sim SF-1\}$. $R_m(k)$ is given by

$$\begin{aligned} R_m(k) &= \frac{1}{\sqrt{SF}} \sum_{t=0}^{SF-1} r_m(t) \exp\left(-j2\pi k \frac{t}{SF}\right) \\ &= \sqrt{\frac{2E_c}{N_t T_c}} H_m(k) \sum_{u=0}^{U-1} d_u C_u(k) + \Pi_m(k), \end{aligned} \tag{4}$$

where $C_u(k)$ is the kth frequency component of $\{\tilde{c}_u(t); t = 0 \sim SF-1\}$, $H_m(k)$ is the composite channel gain obtained by CDTD, and $\Pi_m(k)$ is the kth frequency component of noise, respectively. These are given by

$$\begin{cases} C_u(k) = \dfrac{1}{\sqrt{SF}} \displaystyle\sum_{t=0}^{SF-1} \tilde{c}_u(t) \exp\left(-j2\pi k \frac{t}{SF}\right) \\ H_m(k) = \displaystyle\sum_{n=0}^{N_t-1}\sum_{l=0}^{L-1} h_l^{n\to m} \exp\left(-j2\pi k \frac{\tau_l^{n\to m} + n\Delta}{SF}\right) \\ \Pi_m(k) = \dfrac{1}{\sqrt{SF}} \displaystyle\sum_{t=0}^{SF-1} \eta_m(t) \exp\left(-j2\pi k \frac{t}{SF}\right) \end{cases}. \tag{5}$$

CDTD can increase the number of equivalent paths by transmitting the same data from different antennas after adding different cyclic delays and hence, the CDTD channel can be treated as a composite channel which is the sum of N_t channels. The example of the impulse response of the composite channel $h_m(\tau) = \sum_{n=0}^{N_t-1}\sum_{l=0}^{L-1} h_l^{n\to m}\delta(\tau - n\Delta - \tau_l^{n\to m})$

and the composite channel gain $H_m(k)$ are shown in Fig. 2 and Fig. 3, respectively, for an $L = 4$ path channel when $N_t = 1$ and $N_t = 4$. It can be understood from Fig. 3 that CDTD enhances the degree of frequency-selectivity of the channel. This can be exploited by the use of MMSE-FDE which can achieve larger frequency diversity gain.

3. Joint FDE and Despreading

In this section, first, we show the conventional MMSE-FDE used for DS-CDMA using CDTD [10]–[13] in Sect. 3.1. The joint FDE and despreading is proposed for single-code transmission in Sect. 3.2 and for multi-code transmission in Sect. 3.3. In Sect. 3.4, a theoretical conditional BER analysis is presented for the given channel condition. Figure 4 shows the receiver structure of DS-CDMA using CDTD using the conventional MMSE-FDE and the joint FDE and despreading. By the use of the joint FDE and despreading, all signal processing (equalization, despreading, and diversity combining) can be simultaneously performed in the frequency-domain.

3.1 Conventional MMSE-FDE

The conventional MMSE-FDE and antenna diversity combining are carried out on $R_m(k)$ as

$$\hat{R}(k) = \sum_{m=0}^{N_r-1} R_m(k) W_m(k), \tag{6}$$

where $W_m(k), m = 0 \sim N_r - 1$, is the MMSE-FDE weight which minimizes the mean square error (MSE) between $\hat{R}(k)$ and the frequency component of the transmitted chip sequence $\sum_{u=0}^{U-1} d_u C_u(k)$ and is given by [13]

$$W_m(k) = \frac{H_m^*(k)}{\sum_{m'=0}^{N_r-1} |H_{m'}(k)|^2 + \left(\frac{1}{N_t}\frac{U}{SF}\frac{E_s}{N_0}\right)^{-1}} \tag{7}$$

where E_s/N_0 is the signal energy per symbol-to-AWGN power spectrum density ratio. After MMSE-FDE, the frequency-domain signal $\{\hat{R}(k); k = 0 \sim SF - 1\}$ is transformed by SF-point inverse FFT (IFFT) into a time-domain signal $\{\hat{r}(t); t = 0 \sim SF - 1\}$ as

$$\hat{r}(t) = \frac{1}{\sqrt{SF}} \sum_{k=0}^{SF-1} \hat{R}(k) \exp\left(j2\pi t \frac{k}{SF}\right). \tag{8}$$

Finally, despreading is performed to obtain the decision variable associated with d_u as

$$\begin{aligned}
\hat{d}_u &= \frac{1}{SF}\sum_{t=0}^{SF-1} \hat{r}(t) c_u^*(t) c_{scr}^*(t) \\
&= \sqrt{\frac{2E_c}{N_t T_c}} \left(\frac{1}{SF}\sum_{k=0}^{SF-1}\hat{H}(k)\right) d_u \\
&+ \sqrt{\frac{2E_c}{N_t T_c}} \frac{1}{SF^2} \sum_{t=0}^{SF-1}\sum_{k=0}^{SF-1} \hat{H}(k) \sum_{\substack{\tau=0 \\ \neq t}}^{SF-1} d_u \tilde{c}_u(\tau) \exp\left(j2\pi k \frac{t-\tau}{SF}\right) \tilde{c}_u^*(t) \\
&+ \sqrt{\frac{2E_c}{N_t T_c}} \frac{1}{SF^2} \sum_{t=0}^{SF-1}\sum_{k=0}^{SF-1} \hat{H}(k) \left[\sum_{\substack{\tau=0 \\ \neq t}}^{SF-1}\sum_{\substack{u'=0 \\ \neq u}}^{U-1} d_{u'} \tilde{c}_{u'}(\tau) \exp\left(j2\pi k \frac{t-\tau}{SF}\right)\right] \tilde{c}_u^*(t) \\
&+ \frac{1}{SF}\sum_{t=0}^{SF-1} \frac{1}{\sqrt{SF}} \sum_{k=0}^{SF-1} \hat{\Pi}(k) \exp\left(j2\pi k \frac{t}{SF}\right) \tilde{c}_u^*(t),
\end{aligned} \tag{9}$$

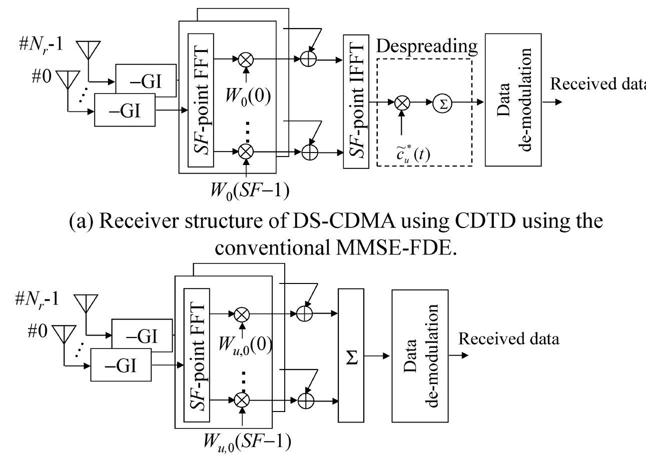

(a) Receiver structure of DS-CDMA using CDTD using the conventional MMSE-FDE.

(b) Receiver structure of DS-CDMA using CDTD using the joint FDE and despreading.

Fig. 4 Receiver structure.

where $\hat{H}(k) = \sum_{m=0}^{N_r-1} H_m(k) W_m(k)$ and $\hat{\Pi}(k) = \sum_{m=0}^{N_r-1} \Pi_m(k) W_m(k)$. In the above, the first, second, third, and forth terms are the desired signal component, the self-code interference component, the inter-code interference component, and the noise component, respectively. The instantaneous signal-to-interference plus noise power ratio (SINR) for the given set of the composite channel gains $\{H_m(k); k = 0 \sim SF - 1\}$ is given by [14]

$$\gamma\left(\frac{E_s}{N_0}, \{H_m(k)\}\right) = \frac{\frac{2}{N_t}\frac{E_s}{N_0}\left|\frac{1}{SF}\sum_{k=0}^{SF-1}\hat{H}(k)\right|^2}{\frac{1}{SF}\sum_{k=0}^{SF-1}\sum_{m'=0}^{N_r-1}|W_{m'}(k)|^2 + \left(\frac{U}{N_t}\frac{E_c}{N_0}\right) \cdot \left\{\frac{1}{SF}\sum_{k=0}^{SF-1}\left|\hat{H}(k)\right|^2 - \left|\frac{1}{SF}\sum_{k=0}^{SF-1}\hat{H}(k)\right|^2\right\}}. \tag{10}$$

CDTD enhances the frequency-selectivity of the channel and therefore, larger residual ICI is produced after MMSE-FDE. This ICI contains the self-code interference and the inter-code interference, the second term and third term of Eq. (9).

3.2 Joint Frequency-Domain Equalization and Despreading for Single-Code Transmission

For the single-code transmission, the frequency-domain signal $\{R_m(k); k = 0 \sim SF-1\}$ can be expressed as

$$R_m(k) = \left(\sqrt{\frac{2E_c}{N_t T_c}} H_m(k) C_0(k)\right) d_0 + \Pi_m(k). \tag{11}$$

The frequency-domain signal after multiplying $W_m(k)$ and antenna diversity combining is expressed as

$$\begin{aligned}\hat{R}(k) &= \sum_{m=0}^{N_r-1} R_m(k) W_m(k) \\ &= \left(\sqrt{\frac{2E_c}{N_t T_c}} \sum_{m=0}^{N_r-1} H_m(k) W_m(k) C_0(k)\right) d_0 \\ &\quad + \sum_{m=0}^{N_r-1} \Pi_m(k) W_m(k),\end{aligned} \tag{12}$$

where the first term represents the desired signal component and the second term is the noise component. The decision variable is obtained as

$$\begin{aligned}\hat{d}_0 &= \frac{1}{\sqrt{SF}} \sum_{k=0}^{SF-1} \hat{R}(k) \\ &= \sqrt{\frac{2E_c}{N_t T_c}} \left(\frac{1}{\sqrt{SF}} \sum_{m=0}^{N_r-1} \sum_{k=0}^{SF-1} H_m(k) W_m(k) C_0(k)\right) d_0 \\ &\quad + \sum_{m=0}^{N_r-1} \Pi_m(k) W_m(k),\end{aligned} \tag{13}$$

The conditional signal-to-noise power ratio (SNR) after above joint FDE and despreading is given by

$$\gamma\left(\frac{E_s}{N_0}, \{H_m(k)\}\right) = \frac{\dfrac{2}{N_t}\dfrac{E_s}{N_0}\left|\dfrac{1}{SF}\displaystyle\sum_{k=0}^{SF-1} \hat{H}(k) C_0(k)\right|^2}{\dfrac{1}{SF}\displaystyle\sum_{k=0}^{SF-1}\sum_{m'=0}^{N_r-1} |W_{m'}(k)|^2}. \tag{14}$$

Applying the Schwarz inequality for complex-valued numbers [15], the weight which maximizes the SNR is found to be

$$W_m^{MRC}(k) = \{C_0(k) H_m(k)\}^*, \tag{15}$$

which is called the maximal-ratio combining (MRC) weight.

3.3 Joint Frequency-Domain Equalization and Despreading for Multi-Code Transmission

For the multi-code transmission, the frequency-domain signal $\{R_m(k); k = 0 \sim SF-1\}$ can be expressed as Eq. (4). The frequency-domain signal after multiplying the joint FDE and despreading weight $W_{u,m}(k), u = 0 \sim U-1$, and antenna diversity combining is expressed as

$$\begin{aligned}\hat{R}_u(k) &= \sqrt{\frac{2E_c}{N_t T_c}} \sum_{u'=0}^{U-1} \left\{\left(\sum_{m=0}^{N_r-1} H_m(k) W_{u,m}(k) C_{u'}(k)\right) d_{u'}\right\} \\ &\quad + \sum_{m=0}^{N_r-1} \Pi_m(k) W_{u,m}(k).\end{aligned} \tag{16}$$

Equation (16) shows that the frequency-domain signal is a linear sum of simultaneously transmitted U data symbols. For this reason, joint FDE and despreading using the MRC weight increases the inter-code interference resulting from the ICI and hence, degrades the BER performance. Below, we derive two types of MMSE weight that can reduce the inter-code interference.

We define the equalization error $e_u(k)$ at the kth frequency as

$$e_u(k) = \hat{R}_u(k) - d_u \tag{17}$$

and derive the MMSE weight $W_{u,m}^{(1)}(k)$ which minimizes the MSE $E[|e_u(k)|^2]$ for each combination of u and k, where $u = 0 \sim U-1$ and $k = 0 \sim SF-1$. We call this MMSE weight as the MMSE weight type 1. The MMSE weight type 1 can be derived as (see Appendix A)

$$W_{u,m}^{(1)}(k) = \frac{\{C_u(k) H_m(k)\}^*}{\displaystyle\sum_{u'=0}^{U-1} |C_{u'}(k)|^2 \sum_{m'=0}^{N_r-1} |H_{m'}(k)|^2 + \left(\frac{1}{N_t}\frac{1}{SF}\frac{E_s}{N_0}\right)^{-1}}. \tag{18}$$

Using the MMSE weight type 1, all of equalization, despreading, and diversity combining can be simultaneously performed in the frequency-domain as

$$\begin{aligned}\hat{d}_u &= \frac{1}{\sqrt{SF}} \sum_{m=0}^{N_r-1}\sum_{k=0}^{SF-1} R_m(k) W_{u,m}^{(1)}(k) \\ &= \sqrt{\frac{2E_c}{N_t T_c}} \left(\frac{1}{\sqrt{SF}} \sum_{k=0}^{SF-1} C_u(k) \hat{H}(k)\right) d_u \\ &= \sqrt{\frac{2E_c}{N_t T_c}} \frac{1}{\sqrt{SF}} \sum_{k=0}^{SF-1} \hat{H}(k) \sum_{\substack{u'=0 \\ \neq u}}^{U-1} d_{u'} C_{u'}(k) \\ &\quad + \frac{1}{\sqrt{SF}} \sum_{m=0}^{N_r-1}\sum_{k=0}^{SF-1} W_{u,m}^{(1)}(k) \Pi_m(k),\end{aligned} \tag{19}$$

where the first, second, and third terms represent the desired signal component, the inter-code interference component, and the noise component, respectively. The SINR after the above joint FDE and despreading for the given set of the composite channel gains $\{H_m(k); k = 0 \sim SF-1\}$ is given by

$$\gamma\left(\frac{E_s}{N_0}, \{H_m(k)\}\right) = \frac{\dfrac{2}{N_t}\dfrac{E_s}{N_0}\left|\dfrac{1}{SF}\displaystyle\sum_{k=0}^{SF-1} \hat{H}(k) C_u(k)\right|^2}{\dfrac{1}{SF}\displaystyle\sum_{k=0}^{SF-1}\sum_{m'=0}^{N_r-1} \left|W_{u,m'}^{(1)}(k)\right|^2 + \left(\dfrac{1}{N_t}\dfrac{E_s}{N_0}\right)\sum_{\substack{u'=0 \\ \neq u}}^{U-1}\left|\dfrac{1}{SF}\displaystyle\sum_{k=0}^{SF-1} \hat{H}(k) C_{u'}(k)\right|^2}. \tag{20}$$

The second term of the denominator in Eq. (20) represents the residual inter-code interference. From Eqs. (19) and (20), however, the self-code interference is not produced while it is produced in the conventional MMSE-FDE.

The second type of MMSE weight (called MMSE weight type 2), $W_{u,m}^{(2)}(k)$, is derived by taking into account the totality of equalization errors at all u (data stream) and k (frequency), where $u = 0 \sim U-1$ and $k = 0 \sim SF-1$. The frequency-domain signal can be expressed using the matrix form as

$$\mathbf{R}_m = [R_m(0),\ldots,R_m(SF-1)]^T = \sqrt{\frac{2E_c}{N_t T_c}}\mathbf{H}_m\mathbf{C}\mathbf{d} + \mathbf{\Pi}_m, \tag{21}$$

where $\mathbf{H}_m = diag[H_m(0),\ldots,H_m(SF-1)]$ is an $SF\times SF$ diagonal composite channel gain matrix, $\mathbf{C}$ is an $SF\times U$ frequency-domain spreading matrix, $\mathbf{d} = [d_0,\ldots,d_{U-1}]^T$ is the transmitted data symbol vector, and $\mathbf{\Pi}_m = [\Pi_m(0),\ldots,\Pi_m(SF-1)]^T$ is the noise vector. $\mathbf{C}$ is given as

$$\mathbf{C} = \begin{bmatrix} C_0(0) & \cdots & C_{U-1}(0) \\ \vdots & \ddots & \vdots \\ C_0(SF-1) & \cdots & C_{U-1}(SF-1) \end{bmatrix}. \tag{22}$$

In Eq. (21), the concatenation of the spreading process and the propagation channel, $\mathbf{H}_m\mathbf{C}$, can be viewed as an equivalent $SF\times U$ multi-input multi-output (MIMO) channel. An $U\times SF$ MMSE weight matrix Wm can be derived by taking into account the totality of equalization errors at all u and k, where $u = 0 \sim U-1$ and $k = 0 \sim SF-1$, similar to the MIMO signal detection.

We define the equalization error vector $\mathbf{e}$ as

$$\mathbf{e} = \sum_{m=0}^{N_r-1}\mathbf{W}_m\mathbf{R}_m - \sqrt{\frac{2E_c}{N_t T_c}}\mathbf{d}. \tag{23}$$

The MMSE weight matrix $\mathbf{W}_m^{(2)}$, which minimizes the trace $tr[E(\mathbf{e}\mathbf{e}^H)]$ of the covariance matrix of the error vector $\mathbf{e}$, can be derived according to the Wiener theory [16]. We have (see Appendix B)

$$\mathbf{W}_m^{(2)} = \begin{bmatrix} W_{0,m}^{(2)}(0) & W_{0,m}^{(2)}(1) & \cdots & W_{0,m}^{(2)}(SF-1) \\ W_{1,m}^{(2)}(0) & W_{1,m}^{(2)}(1) & \cdots & W_{1,m}^{(2)}(SF-1) \\ \vdots & \vdots & \ddots & \vdots \\ W_{U-1,m}^{(2)}(0) & W_{U-1,m}^{(2)}(1) & \cdots & W_{U-1,m}^{(2)}(SF-1) \end{bmatrix}$$
$$= \mathbf{C}^H\mathbf{H}_m^H\left[\sum_{m'=0}^{N_r-1}\mathbf{H}_{m'}\mathbf{C}\mathbf{C}^H\mathbf{H}_{m'}^H + \left(\frac{1}{N_t}\frac{1}{SF}\frac{E_s}{N_0}\right)^{-1}\mathbf{I}\right]^{-1}, \tag{24}$$

where $\mathbf{I}$ is an $SF\times SF$ unit matrix. The decision variable for the data symbol in the uth stream is obtained as

$$\hat{d}_u = \sum_{m=0}^{N_r-1}\sum_{k=0}^{SF-1}W_{u,m}^{(2)}R_m(k) \tag{25}$$
$$= \sqrt{\frac{2E_c}{N_t T_c}}\bar{H}_{u,u}d_u + \sqrt{\frac{2E_c}{N_t T_c}}\sum_{\substack{u'=0\\ \neq u}}^{U-1}\bar{H}_{u,u'}d_{u'} + \sum_{m=0}^{N_r-1}\sum_{k=0}^{SF-1}W_{u,m}^{(2)}\Pi_m(k),$$

where $\bar{H}_{u,u'}$ is the (u, u')th element of $\bar{\mathbf{H}} = \sum_{m=0}^{N_r-1}\mathbf{W}_m^{(2)}\mathbf{H}_m^H\mathbf{C}$. The first, second, and third terms of Eq. (25) represent the desired signal component, the inter-code interference component, and the noise component, respectively. The SINR after the above joint FDE and despreading for the given set of the composite channel gains $\{H_m(k); k = 0 \sim SF-1\}$ is given by

$$\gamma\left(\frac{E_s}{N_0},\{H_m(k)\}\right) = \frac{\frac{2}{N_t}\frac{E_s}{N_0}\left|\bar{H}_{u,u}\right|^2}{\sum_{k=0}^{SF-1}\sum_{m'=0}^{N_r-1}\left|W_{u,m'}^{(2)}(k)\right|^2 + \left(\frac{1}{N_t}\frac{E_s}{N_0}\right)\sum_{\substack{u'=0\\ \neq u}}^{U-1}\left|\bar{H}_{u,u'}\right|^2}. \tag{26}$$

3.4 BER Analysis

We consider QPSK, 16QAM, and 64QAM for data modulation. It can be understood from Eqs. (19) and (25) that the decision valuable $\hat{d}$ is a random variable with mean the first term of Eqs. (18) and (25). Since the residual ICI component which is the second term in Eqs. (18) and (25) can be approximated as a zero-mean complex-valued Gaussian noise, the sum of the second term and the third term in Eqs. (18) and (25) can be treated as a new zero-mean complex-valued Gaussian noise μ [14]. In this case, the SINR in Eqs. (19) and (26) can be regarded as the equivalent SNR. Therefore, the theoretical conditional BER (it is an exact expression for QPSK) of the data symbol in the uth stream for the given set of the composite channel gains $\{H_m(k); k = 0 \sim SF-1\}$ is given as [1]

$$p_b\left(\frac{E_s}{N_0},\{H_m(k)\}\right) \cong \begin{cases} \frac{1}{2}erfc\left[\sqrt{\frac{1}{4}\gamma\left(\frac{E_s}{N_0},\{H_m(k)\}\right)}\right], & \text{QPSK} \\ \frac{3}{8}erfc\left[\sqrt{\frac{1}{20}\gamma\left(\frac{E_s}{N_0},\{H_m(k)\}\right)}\right], & \text{16QAM} \\ \frac{7}{24}erfc\left[\sqrt{\frac{1}{84}\gamma\left(\frac{E_s}{N_0},\{H_m(k)\}\right)}\right], & \text{64QAM} \end{cases}. \tag{27}$$

where $erfc[x] = (2/\sqrt{\pi})\int_x^\infty \exp(-t^2)dt$ is the complementary error function. The theoretical average BER can be numerically evaluated by averaging Eq. (27) over all possible realizations of $\{H_m(k); k = 0 \sim SF-1\}$.

4. Numerical and Simulation Results

The condition for the numerical evaluation of the theoretical average BER and the computer simulation is shown in Table 1. The Walsh-Hadamard sequences are used as the orthogonal spreading codes and a long PN sequence with a repetition period of 4095 chips is used as the scramble sequence. We assume a block length and FFT window size equal to the spreading factor SF and a GI length of $N_g = 16$. The channel is assumed to be a chip-spaced $L = 16$-path frequency-selective block Rayleigh fading channel having exponential power delay profile with the path decay factor α. Ideal channel estimation is assumed.

The numerical evaluation of the theoretical average BER is done by Monte-Carlo numerical computation method as follows. The set of path gains $\{h_l^{n\to m}; n = 0 \sim N_t - 1, m = 0 \sim N_r - 1, l = 0 \sim L - 1\}$ is generated for obtaining $\{H_m(k); m = 0 \sim N_r - 1, k = 0 \sim SF - 1\}$ using Eq. (5) and then $\{W_m^{MRC}; m = 0 \sim N_r - 1, l = 0 \sim L - 1\}$ or $\{W_{u,m}^{(1)\text{or}(2)}(k); u = 0 \sim U-1, m = 0 \sim N_r-1, k = 0 \sim SF-1\}$ using Eq. (15) or Eqs. (18) and (24). The conditional BER for the given average received E_s/N_0 is computed using Eq. (27). This is repeated sufficient number of times to obtain the theoretical average BER. The computer simulation is also carried out to obtain the average BER to confirm the validity of the theoretical analysis.

4.1 Single-Code Transmission

The theoretical and computer-simulated average BER performances of CDTD for the single-code case with joint FDE and despreading using the MRC weight are plotted in Fig. 5 as a function of average received bit energy-to-noise power spectrum density ratio $E_b/N_0(= (E_s/N_0)(SF + N_g)/\log_2 M)$, where M is the modulation level. $N_t = 4$ is assumed. For the conventional MMSE-FDE, only the theoretical BER performance is plotted. Also plotted is the theoretical lower bound [13]. A fairly good agreement between theoretical and computer simulated results is seen for joint FDE and despreading using the MRC weight.

Table 1 Simulation condition.

Transmitter	No. of transmit antennas	N_t = 1–4
	Modulation	QPSK, 16QAM, 64QAM
	Block length	SF
	GI	$N_g = 16$
	Spreading sequence	Walsh sequence
	Spreading factor	$SF = 64$
	No. of parallel codes	U = 1–64
	Scramble code	Long PN sequence
Channel	Fading type	Frequency-selective block Rayleigh
	Power delay profile	L = 16-path ecponential power delay profile
	Decay factor	α = 6(dB)
Receiver	FFT block size	SF
	FDE	MMSE, MRC
	Channel estimation	Ideal

When QPSK data modulation ($M = 4$) is used, the ICI is not significant even in the conventional MMSE-FDE and therefore, only a slight performance difference is seen between the joint FDE and despreading and the conventional MMSE-FDE. For higher modulation level (i.e., $M = 16, 64$), since the Euclidian distance between the symbol constellation points becomes smaller, the BER performance using the conventional MMSE-FDE degrades due to the residual ICI. However, since the joint FDE and despreading does not produce the residual ICI at all, better BER performance can be achieved. The performance improvement gets larger for higher level modulation. When the joint FDE and

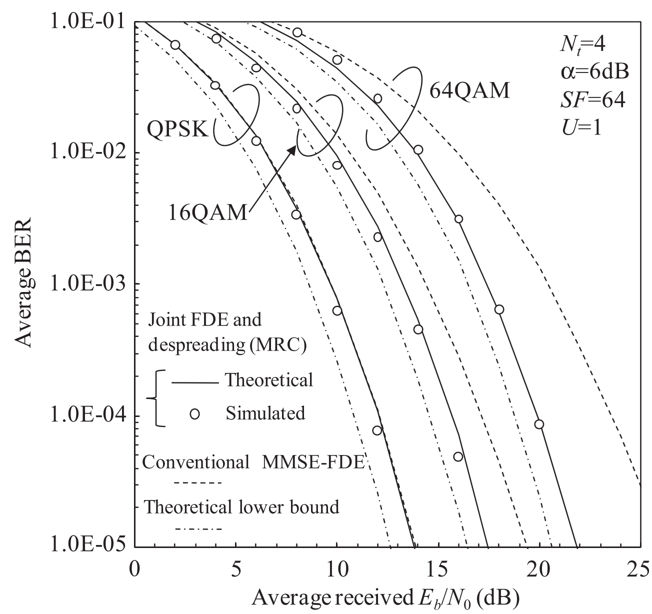

(a) N_r=1

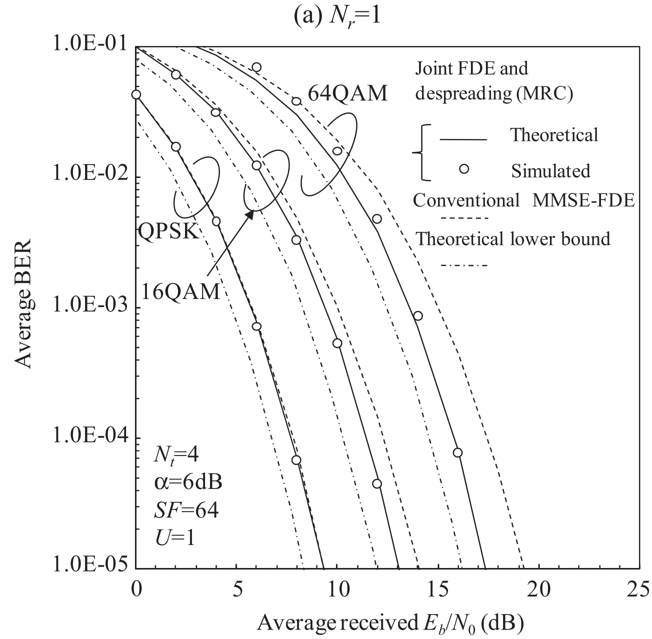

(b) N_r=2

Fig. 5 Theoretical and simulated BER performance with joint FDE and despreading for single-code transmission.

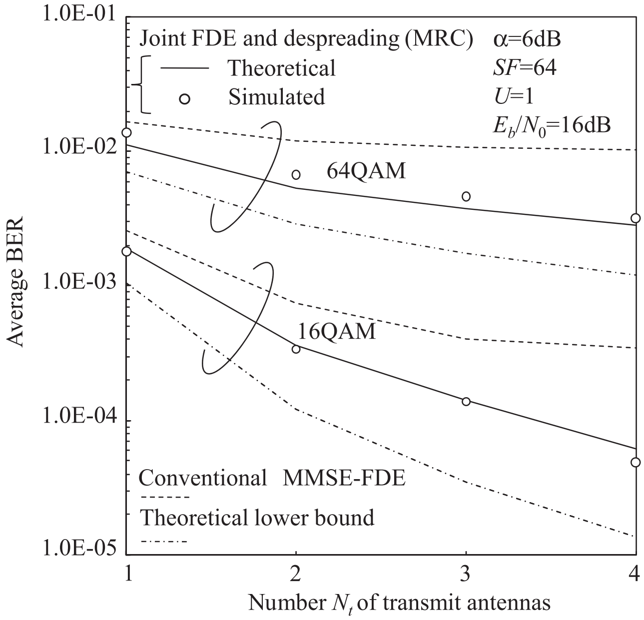

Fig. 6 Impact of the number N_t of transmit antennas for single-code transmission.

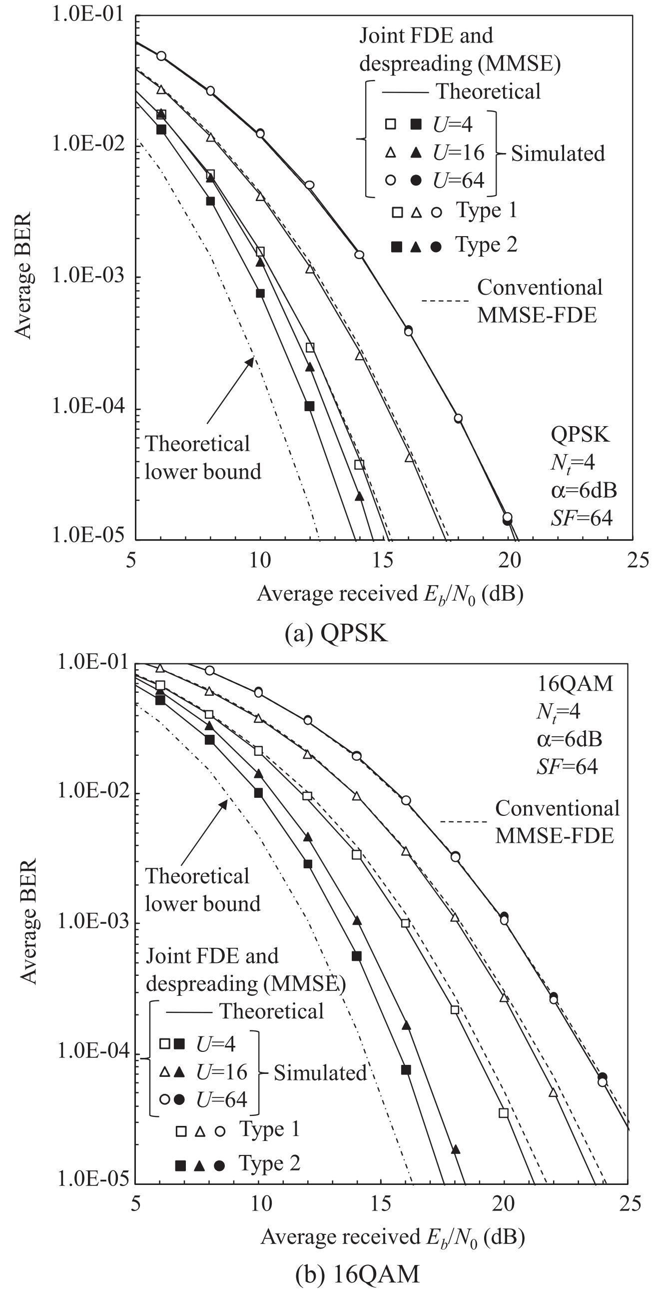

Fig. 7 Theoretical and simulated BER performances with joint FDE and despreading for multi-code transmission.

despreading is used, the BER performance approaches the theoretical lower bound (a degradation from the theoretical lower bound is due to the GI insertion loss (0.97 dB)). When $N_r = 2$, since the residual ICI can be suppressed by the received diversity effect, the BER performance improvement is reduced.

Figure 6 plots the theoretical and computer-simulated average BER performances of CDTD for the single-code case using the joint FDE and despreading with the number of transmit antenna N_t as a parameter for 16QAM and 64QAM. Only the theoretical BER performance is plotted for the conventional MMSE-FDE. CDTD using the conventional MMSE-FDE can improve the BER performance by increasing the number of transmit antennas. However, the residual ICI limits the BER performance improvement. On the other hand, since the joint FDE and despreading does not produce the ICI at all even if the number of transmit antennas increases, almost the same frequency diversity gain as the lower bound can be achieved and the BER performance is improved compared to the conventional MMSE-FDE.

4.2 Multi-Code Transmission

The theoretical and computer-simulated average BER performances of CDTD for the multi-code case with joint FDE and despreading are plotted in Fig. 7 as a function of E_b/N_0 with the code multiplexing order U as a parameter. $N_t = 4$ is assumed. For the conventional MMSE-FDE, only the theoretical BER performance is plotted. A fairly good agreement between theoretical and computer simulated results is seen for joint FDE and despreading. Joint FDE and despreading using MMSE weight type 1 does not produce the self-code interference, but cannot eliminate the inter-code interference and therefore, it can achieve only slightly better BER performance than the conventional MMSE-FDE. However, the MMSE weight type 1 has lower computational complexity than the conventional MMSE-FDE (this will be discussed in the next subsection). As U increases, the BER performance degrades due to the increased residual inter-code interference because the MMSE weight type 1 is designed to minimize the MSE at each frequency individually.

Joint FDE and despreading using the MMSE weight type 2 can significantly improve the BER performance when $U = 4$ and 16. When $U = 64$, however, the MMSE weight type 2 achieves the BER performance identical to

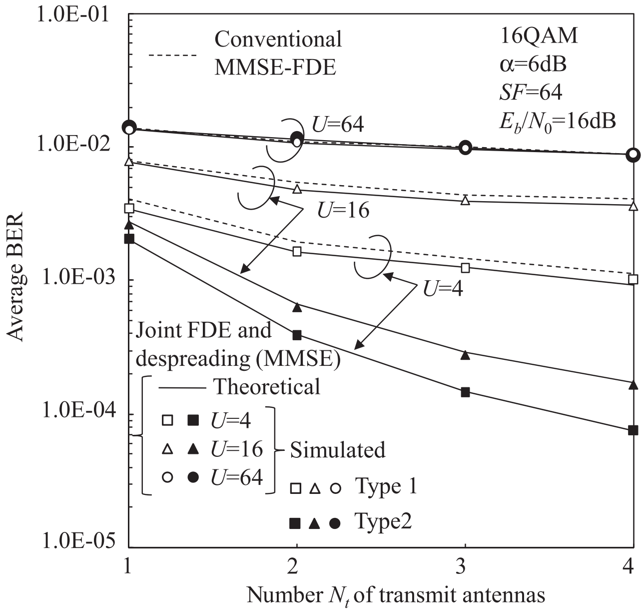

Fig. 8 Impact of the number N_t of transmit antennas for multi-code transmission.

the MMSE weight type 1. This is because when $U = SF$, off diagonal elements of $\mathbf{CC}^H$ become zero and as a consequence, the MMSE weight type 2 reduces to the MMSE weight type 1.

Figure 8 plots the theoretical and computer-simulated average BER performances of CDTD for the multi-code case using the joint FDE and despreading with the number of transmit antennas, N_t, as a parameter. 16QAM data modulation is assumed. Only the theoretical BER performance is plotted for the conventional MMSE-FDE. By increasing the number of transmit antennas, N_t, the achievable BER decreases. However, joint FDE and despreading using the MMSE weight type 1 can only slightly reduce the BER similar to the conventional MMSE-FDE. On the other hand, joint FDE and despreading using the MMSE weight type 2 can reduce the BER much faster by increasing N_t.

4.3 Computational Complexity

The computational complexity of the proposed joint FDE and despreading is compared with that of conventional MMSE-FDE. The complexity here is defined as the number of complex multiply operations required in FDE (including FFT/IFFT) and despreading. In this paper, the binary spreading codes are assumed for the sake of simplicity. However, it should be noted that complex-valued spreading codes are used in practical CDMA mobile communications systems [17]; therefore, complex-valued multiply operation is necessary even in time-domain despreading. So, we assume the complex multiply operation in the time-domain also in the case of conventional MMSE-FDE.

We assume the frequency components of the spreading sequence, $\{C_u(k); k = 0 \sim SF-1\}$, is known to the receiver. Since the conventional MMSE-FDE requires FFT, weight multiplication, IFFT, and despreading, the number of complex multiply operations becomes $(N_r+1)(SF\log_2 SF+SF)$. However, the proposed joint FDE and despreading does not require IFFT and therefore, its computational complexity can be reduced and becomes $N_r(SF\log_2 SF + 2SF)$ for the MMSE weight type 1 while it becomes $U^3 + N_r \cdot SF \cdot U^2 + N_r \cdot SF \cdot U + N_r \cdot SF + N_r \cdot SF \log_2 SF$ for the MMSE weight type 2 (this is because $U \times U$ matrix inversion and matrix multiplication are required). When $N_r = 1(2)$, the computational complexity of joint FDE and despreading using MMSE weight type 1 is about 57(76)% of conventional MMSE-FDE. On the other hand, the computational complexity of joint FDE and despreading using MMSE weight type 2 is 2 (38) times that of conventional MMSE-FDE when $U = 4(16)$. The use of MMSE weight type 1 can reduce the computational complexity, but it can improve the BER performance only slightly. On the other hand, the use of MMSE weight type 2 can significantly improve the BER performance at the cost of increased complexity compared to the MMSE weight type 1 and conventional MMSE-FDE.

5. Conclusions

In this paper, we proposed the joint use of FDE and despreading for single- and multi-code DS-CDMA using CDTD in the frequency-domain. We derived the theoretical conditional BER for the given channel condition and evaluated the achievable average BER by Monte-Calro numerical computation method. The BER analysis was confirmed by computer simulation of the signal transmission. We showed that, in the case of single-code transmission, the joint FDE and despreading using the MRC weight completely suppresses ICI and hence provides better BER performance than the conventional MMSE-FDE. We also showed that, in the case of multi-code trans-mission, joint FDE and despreading using the MMSE weight type 1 can achieve only slightly better BER performance than the conventional MMSE-FDE. Joint FDE and despreading using the MMSE weight type 2 can achieve significantly better BER performance than using the MMSE weight type 1 at the cost of increased complexity.

Acknowledgment

The authors would like to thank the anonymous re-viewers for their valuable comments and suggestions.

References

[1] J.G. Proakis, Digital communications, 2nd ed., McGraw-Hill, 1995.
[2] F. Adachi, M. Sawahashi, and H. Suda, "Wideband DS-CDMA for next generation mobile communications sys-tems," IEEE Trans. Commun., vol.36, no.9, pp.56–69, Sept. 1998.
[3] F. Adachi, D. Garg, S. Takaoka, and K. Takeda, "Broadband CDMA techniques," IEEE Wireless Commun. Mag., vol.12, no.2, pp.8–18, April 2005.
[4] D. Falconer, S.L. Ariyavisitakul, A. Benyamin-Seeyar, and B.

Edison, "Frequency domain equalization for single-carrier broadband wireless systems," IEEE Commun. Mag., vol.40, no.4, pp.58–66, April 2002.

[5] I. Martoyo, G.M. A. Sessler, J. Luber, and F.K. Jondral, "Comparing equalizers and multiuser detections for DS-CDMA downlink systems," Proc. IEEE VTC 2004 Spring, pp.1649–1653, May 2004.

[6] F.W. Vook, T.A. Thomas, and K.L. Baum, "Cyclic-prefix CDMA with antenna diversity," Proc. IEEE VTC 2002 Spring, pp.1002–1006, May 2002. IEEE 64th Veh. Technol. Conf. (VTC2006-Fall), pp.1–5, Montreal, Canada, Sept. 2006.

[7] T. Itagaki and F. Adachi, "Joint frequency-domain equalization and antenna diversity combining for orthogonal multicode DS-CDMA signal transmissions in a frequency-selective fading channel," IEICE Trans. Commun., vol.E87-B, no.7, pp.1954–1963, July 2004.

[8] G. Bauch and J.S. Malik, "Parameter optimization, interleaving and multiple access in OFDM with cyclic delay diversity," Proc. 59th IEEE VTC, vol.1, pp.505–509, Miran, Italia, May 2004.

[9] Gerhard Bauch, "Capacity optimization of cyclic delay diversity," Proc. 60th IEEE VTC, vol.3, pp.1802–1824, Los Angeles, CA, U.S.A., Sept. 2004.

[10] R. Kawauchi, K. Takeda, and F. Adachi, "Application of cyclic delay transmit diversity to DS-CDMA using frequency-domain equalization," IEICE Technical Report, RCS2004-392, March 2005.

[11] R. Kawauchi, K. Takeda, and F. Adachi, "Performance comparison of DS- and MC-CDMA using cyclic delay transmit diversity and frequency-domain equalization," Proc. IEICE Gen. Conf. 2005, B-5-14, March 2005.

[12] R. Kawauchi, K. Takeda, and F. Adachi, "Space-time cyclic delay transmit diversity for a multi-code DS-CDMA signal with frequency-domain equalization," IEICE Trans. Commun., vol.E90-B, no.3, pp.591–596, March 2007.

[13] K. Takeda, Y. Kojima, and F. Adachi, "Transmit diversity for DS-CDMA/MMSE-FDE with frequency-domain ICI cancellation," Proc. 67th IEEE VTC, vol.1, pp.1057–1061, Marina Bay, Singapore, May 2008.

[14] F. Adachi and K. Takeda, "Bit error rate analysis of DS-CDMA with joint frequency-domain equalization and antenna diversity combining," IEICE Trans. Commun., vol.E87-B, no.10, pp.2991–3002, Oct. 2004.

[15] M. Schwartz, W.R. Bennett, and S. Stein, Communication systems and techniques, McGraw-Hill, New York, 1966.

[16] S. Haykin, Adaptive Filter Theory, 4th ed., Prentice Hall, 1996.

[17] 3GTS 25.213 version 3.3.0, "Spreading and Modulation (FDD)," 3GPP TSG-RAN, 2000-06.

Appendix A: Derivation of MMSE Weight Type 1 for Multi-Code DS-CDMA

The equalization error $e_u(k)$ is defined as Eq. (17). Using Eq. (16), $e_u(k)$ is given by

$$\begin{aligned} e_u(k) &= \hat{R}_u(k) - d_u \\ &= \sqrt{\frac{2E_c}{N_t T_c}} \sum_{u'=0}^{U-1} \left\{ \left(\sum_{m=0}^{N_r-1} H_m(k) W_{u,m}(k) C_{u'}(k) \right) d_{u'} \right\} \\ &\quad + \sum_{m=0}^{N_r-1} \Pi_m(k) W_{u,m}(k) - d_u. \end{aligned} \tag{A·1}$$

Since $\Pi_m(k)$ is a zero-mean complex-valued Gaussian noise having variance $2N_0/T_c$, the mean square error is given by

$$E[|e_u(k)|^2] = \sum_{u'=0}^{U-1} \left| \sqrt{\frac{2E_c}{N_t T_c}} \sum_{m=0}^{N_r-1} H_m(k) W_{u,m}(k) C_{u'}(k) - 1 \right|^2 + \frac{2N_0}{T_c} \sum_{m=0}^{N_r-1} |W_{u,m}(k)|^2. \tag{A·2}$$

The MMSE weight $W_{u,m}(k)$ is the one that satisfies $\partial E[|e_u(k)|^2]/\partial W_{u,m}(k) = 0$. From Eq. (A·2), we have

$$\begin{aligned} \frac{\partial E[|e_u(k)|^2]}{\partial W_{u,m}(k)} &= \frac{2E_c}{N_t T_c} W_{u,m}^*(k) \sum_{u'=0}^{U-1} |C_{u'}(k)|^2 \sum_{m'=0}^{N_r-1} |H_{m'}(k)|^2 \\ &\quad + \frac{2N_0}{T_c} W_{u,m}^*(k) - \sqrt{\frac{2E_c}{N_t T_c}} C_u(k) H_m(k). \end{aligned} \tag{A·3}$$

Finally, the MMSE weight is obtained as

$$W_{u,m}^{(1)}(k) = \frac{\{C_u(k) H_m(k)\}^*}{\sum_{u'=0}^{U-1} |C_{u'}(k)|^2 \sum_{m'=0}^{N_r-1} |H_{m'}(k)|^2 + \left(\frac{1}{N_t} \frac{1}{SF} \frac{E_s}{N_0} \right)^{-1}}. \tag{A·4}$$

Appendix B: Derivation of MMSE Weight Type 2 for Multi-Code DS-CDMA

The MMSE weight type 2 minimizes the trace $trE[\mathbf{e}\mathbf{e}^H]$ of the covariance matrix of the equalization error vector $\mathbf{e}$ defined as Eq. (23). Using Eq. (21), $\mathbf{e}$ is given by

$$\begin{aligned} \mathbf{e} &= \sum_{m=0}^{N_r-1} \mathbf{W}_m \mathbf{R}_m - \sqrt{\frac{2E_c}{N_t T_c}} \mathbf{d} \\ &= \sqrt{\frac{2E_c}{N_t T_c}} \sum_{m=0}^{N_r-1} (\mathbf{W}_m \mathbf{H}_m \mathbf{C} - \mathbf{I}) \mathbf{d} + \sum_{m=0}^{N_r-1} \mathbf{W}_m \mathbf{\Pi}_m. \end{aligned} \tag{A·5}$$

The covariance matrix of $\mathbf{e}$ is given by

$$\begin{aligned} E[\mathbf{e}\mathbf{e}^H] &= \frac{2E_c}{N_t T_c} \left(\sum_{m=0}^{N_r-1} \mathbf{W}_m \mathbf{H}_m \mathbf{C} - \mathbf{I} \right) \left(\sum_{m=0}^{N_r-1} \mathbf{W}_m \mathbf{H}_m \mathbf{C} - \mathbf{I} \right)^H \\ &\quad + \frac{2N_0}{T_c} \sum_{m=0}^{N_r-1} \mathbf{W}_m \mathbf{W}_m^H. \end{aligned} \tag{A·6}$$

The MMSE weight $\mathbf{W}_m$ is the one that satisfies $\partial tr(E[\mathbf{e}\mathbf{e}^H])/\partial \mathbf{W}_m = 0$. The following MMSE weight can be derived according to the Wiener theory [16].

$$\mathbf{W}_m^{(2)} = \mathbf{C}^H \mathbf{H}_m^H \left[\sum_{m'=0}^{N_r-1} \mathbf{H}_{m'} \mathbf{C} \mathbf{C}^H \mathbf{H}_{m'}^H + \left(\frac{1}{N_t} \frac{1}{SF} \frac{E_s}{N_0} \right)^{-1} \mathbf{I} \right]^{-1}. \tag{A·7}$$

Tetsuya Yamamoto received his B.S. degree in Electrical, Information and Physics Engineering from Tohoku University, Sendai, Japan, in 2008. Currently he is a graduate student at the Department of Electrical and Communications Engineering, Tohoku University. His research interests include frequency-domain equalization for direct sequence CDMA.

Kazuki Takeda received his B.S. and M.S. degree in communications engineering from Tohoku University, Sendai, Japan, in 2006 and 2008. Currently he is a Japan Society for the Promotion of Science (JSPS) research fellow, studying toward his Ph.D. degree at the Department of Electrical and Communications Engineering, Graduate School of Engineering, Tohoku University. His research interests include precoding and channel equalization techniques for mobile communication systems. He was a recipient of the 2007 IEICE RCS (Radio Communication Systems) Active Research Award.

Fumiyuki Adachi received the B.S. and Dr.Eng. degrees in electrical engineering from Tohoku University, Sendai, Japan, in 1973 and 1984, respectively. In April 1973, he joined the Electrical Communications Laboratories of Nippon Telegraph & Telephone Corporation (now NTT) and conducted various types of research related to digital cellular mobile communications. From July 1992 to December 1999, he was with NTT Mobile Communications Network, Inc. (now NTT DoCoMo, Inc.), where he led a research group on wideband/broadband CDMA wireless access for IMT-2000 and beyond. Since January 2000, he has been with Tohoku University, Sendai, Japan, where he is a Professor of Electrical and Communication Engineering at the Graduate School of Engineering. His research interests are in CDMA wireless access techniques, equalization, transmit/receive antenna diversity, MIMO, adaptive transmission, and channel coding, with particular application to broadband wireless communications systems. From October 1984 to September 1985, he was a United Kingdom SERC Visiting Research Fellow in the Department of Electrical Engineering and Electronics at Liverpool University. He is an IEICE Fellow and was a co-recipient of the IEICE Transactions best paper of the year award 1996 and again 1998 and, also a recipient of Achievement award 2003. He is an IEEE Fellow and was a co-recipient of the IEEE Vehicular Technology Transactions best paper of the year award 1980 and again 1990 and also a recipient of Avant Garde award 2000. He was a recipient of Thomson Scientific Research Front Award 2004.